JETIR.ORG ISSN: 2349-5162 | ESTD Year : 2014 | Monthly Issue
JOURNAL OF EMERGING TECHNOLOGIES AND INNOVATIVE RESEARCH (JETIR)
An International Scholarly Open Access, Peer-reviewed, Refereed Journal

Objective Contrast Evaluation in Mammograms: The Carneiro Contrast Index Approach

[1]Pedro Cunha Carneiro, [1]Anna Carolina Falanga Brenha, [1]Ana Claudia Patrocínio

[1]Faculty of Electrical Engineering,
[1]Federal University of Uberlândia, Uberlândia, Brazil

Abstract : Enhancing the quality of digital breast images is crucial for improving the visualization and identification of breast lesions. Digital image processing techniques play a fundamental role in contrast enhancement, which aids in distinguishing fibroglandular and cancerous tissues, reducing diagnostic subjectivity. Subtle indicators of breast cancer, such as small masses and microcalcifications, can be challenging to detect in low-dose 2D mammograms, where noise further complicates lesion differentiation. Studies highlight the importance of integrating noise filtering and contrast enhancement methods to improve image clarity. The effectiveness of contrast enhancement is often evaluated through qualitative visual inspection, which remains subjective. Consequently, various quantitative contrast performance measures, including variance, MSSIM (Mean Structural Similarity Index Measure), and PSNR (Peak Signal-to-Noise Ratio), have been proposed, though they do not always align with visual perception. Signal-to-Noise Ratio (SNR) and Enhancement Measure Evaluation (EME) are widely used contrast quantification metrics, yet they present limitations when applied to mammographic images due to their dependence on specific object characteristics or predefined regions of interest. To address the need for a global metric capable of objectively assessing contrast enhancement across an entire image, this study introduces the Carneiro Contrast Index (CCI). CCI computes local contrast through a 3x3 kernel, generating a contrast map that highlights regions of high and low contrast. The arithmetic mean of standard deviation values from this matrix provides a single global contrast index. Unlike EME, which requires region-of-interest selection, CCI enables whole-image analysis, ensuring greater reproducibility and applicability across different imaging conditions. The proposed metric aligns with radiologists' visual assessments and established contrast measures, demonstrating its robustness in evaluating contrast enhancement techniques. Future research will explore the integration of CCI with deep learning models and automated diagnostic systems, further enhancing breast cancer detection accuracy and efficiency.

Index Terms **- 2D Mammogram, Contrast Evaluation, Imaging Processing, Medical Imaging**

I. INTRODUCTION

As a way to improve digital breast images quality, the usage of digital processing techniques is essential, in order to enhance contrast and facilitate breast lesions visualization and identification of breast lesions. The primary objective of these techniques is to enhance image quality, facilitating more precise object differentiation in the examination [1].

Subtle indicators of breast cancer, including small nodules or microcalcifications, may be challenging for radiologists to identify due to the low X-ray doses used in 2D mammograms [2]. The contrast between fibroglandular and cancerous tissues can be present on breast images, however, under the human visual threshold, which considerably increases diagnostic subjectivity. Saunders et al. [3] had evidenced that the greater the noise presence on a mammographic image, the higher is the difficulty to notice and distinguish different objects in it, such as microcalcifications, making it also harder to differentiate benign and malignant masses. Therefore, numerous studies in the literature emphasize the significance of integrating noise filtering with contrast enhancement techniques in imaging [4-10]. In this way, digital processing techniques are essential for enhancing image contrast by highlighting specific objects against the background and improving visual perception, which is inherently subjective.

Contrast enhancement techniques can be classified as direct or indirect. In the direct ones, a contrast measurement criteria is setted and applied directly in the image, unlike in the indirect ones, where the image's contrast is not directly manipulated, but rather the histogram is modified, to further change the contrast [11].

A potential approach to assessing the effectiveness of a contrast enhancement technique is visual inspection, though this qualitative method remains inherently subjective. Thus, some quantitative contrast performance measures that can be applied after digital processing are found in literature, in order to compare the original images with the ones with the contrast enhancement post-processing.

Some techniques for contrast quantification are widely used, such as variance, MSSIM or PSNR, but they don't always agree with visual analysis [12].The Signal-Noise Ratio (SNR) is a contrast measure that does not depend on the analyzed object's size, it

is a quantification of signal in the presence of noise, being the difference between the gray scale average of the region of interest of the signal ($\underline{X}_S$) and the region of interest of the background ($\underline{X}_F$), considering also σ_S e σ_F, the standard deviations of the signal and the background of the region of interest, respectively [13].

SNR is a good metric to describe signal amplitude compared to the image noise. Once the calculation is computed from the difference between the signal and background's region means, this measure is mostly applied when using objects that generate a homogeneous signal level [14]. Though, in mammographic images, SNR is commonly calculated with an aluminum object positioned in polymethacrylate (PMMA), which makes the calculus harder in real mammograms.

Another well-known quantitative contrast metric is the Measure of Enhancement (EME) [15]. According to the authors, the image improvement after digital processing is generally tricky to measure, also due the difficulty to scale visual perception. Considering the shades of gray of a mammogram, $I^{w}_{max;k,l}$ e $I^{w}_{min;k,l}$ represent the maximums and $X(n,m)$ the minimums of the image, inside a $w_{k,l}$ block. The image must me split in k_1k_2, in $l_1 \, x \, l_2$ sized $w_{k,l}(i,j)$ blocks, and $\{\Phi\}$ must be a determined class of orthogonal transformations.

This measure is related to Weber's Law for the human visual system, which tries to measure human responses to physical stimulation. The higher the EME value for a certain region of interest, the higher the contrast between the pixels in this region, since the difference between its minimums and maximums is also higher. Such metric aims to validate contrast objectively, once it considers the high dependency between processed pixels and its neighbors.

A limitation of employing EME for contrast enhancement quantification in mammographic images is its dependence on selecting a region of interest. This implies a local metric, which cannot mean a consistent result for the whole image, once the measurement depends exclusively on the selected region. Consequently, if the region of interest is too large, aiming to display a result closer to a whole-image analysis, the computational cost is increased.

Considering the necessity for a global metric capable of quantitatively assessing contrast by analyzing multiple image regions, this study proposes the development of a contrast quantification metric for mammographic images following contrast enhancement processing. Thus, an average local contrast index based on local standard deviations was implemented, named Carneiro Contrast Index (CCI).

II. METHODOLOGY

The Carneiro Contrast Index

The proposed index [12] computes the standard deviation values within a 3x3 kernel that traverses all image pixels, producing a contrast map that represents the standard deviation between the central pixel and its eight neighboring pixels. In this way, after the kernel has gone through the whole image, calculating the local standard deviations in 3x3 sized regions, a resultant matrix with the standard deviation values is returned, with the same size as the original input image.

The resulting matrix inherently provides a qualitative representation by visually depicting the standard deviation value. Brighter regions generally indicate areas of higher contrast in the original image (higher standard deviation), whereas darker regions correspond to lower standard deviation values and, consequently, reduced contrast. Figure 1 exemplifies the standard deviation resultant matrix for two images: an original one (without any processing) and its processed version, with the CLAHE technique.

Through Figure 1, it can be observed that the map for the processed image presents lighter shades of gray, suggesting higher contrast when compared to the original image, in which the resultant map presents darker shades, that being lower standard deviation values. In the original image's map, the presence of lighter pixels only in the breast edges are noticed (background/breast interface).

After the creation of the resultant standard deviation matrix, its arithmetic mean ($\underline{x}$) is calculated, resulting in a single CCI value for the image. For better comparison effects, the images must be normalized between 0 and 1, dividing the pixel values by the maximum scale bottom value. Thus, for 12-bit images, all pixel values in the original matrix must be divided by 4095, making a normalized pixel value equals one only when the original pixel equals 4095. Normalization is essential for comparing images with varying contrast resolutions, given that tomosynthesis scans use 10-bit images (maximum intensity 1023), whereas digital mammograms utilize 12-bit images (maximum intensity 4095), depending on the acquisition system.

To enhance interpretability, the index value is multiplied by 1000, as the original index values tend to be very small due to the normalization process. The higher the contrast index, the greater is the global contrast of the analyzed image, based on local contrasts (by region). Equation 1 defines the final CCI computation, considering only standard deviation values greater than zero, which correspond to regions where contrast modifications occurred.

Figure 1 - Example of resultant standard deviation matrixes (maps) between an original image, with no processing, and a processed image.

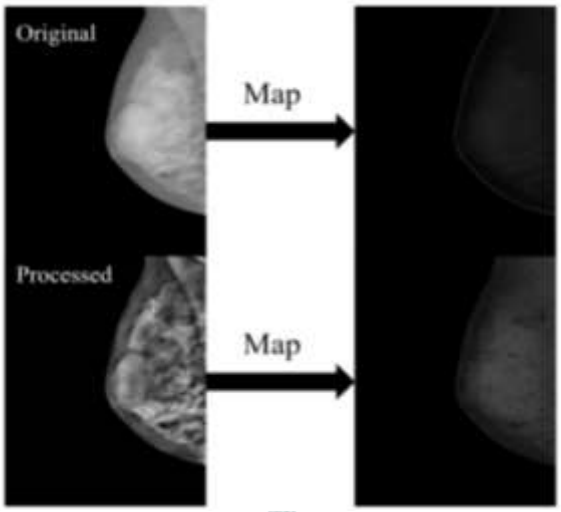

Source: Modified from [12].

Equation 1: CCI computing formula [12].

$$CCI(x,y) = \frac{1}{numel}\underbrace{\left[\sum_{m=-1}^{1}\sum_{n=-1}^{1}(f(x+m,y+n)-\mu_k)^2\right]^{1/2}}_{=\,dp_i} x1000 \quad (1)$$

$$\text{If } dp_i > 0;\ CCI(x,y) = \frac{1}{numel}\,dp_i$$

$$\text{If } dp_i = 0;\ CCI(x,y) = 0$$

where:

- $f(x,y)$ = Image of size m x n pixels;
- $numel$ = Number of elements with standard deviation results higher than zero (for calculating standard deviation matrix arithmetic mean);
- μ_k = Arithmetic mean of the pixels inside the kernel being analysed (used for calculating local standard deviation);

In Figure 2, the original image is normalized, and a scrolling 3x3 kernel runs through the matrix, obtaining the local standard deviations. Finally, the arithmetic mean of the resultant pixels, that are higher than zero, is calculated. It is important to highlight that, in Figure 2, the edge pixels were mirrored in order to fulfill the 3x3 kernel. In this case, it is presumed that the kernel (in red) has already run through the entire image, therefore, all the standard deviation values were properly determined. For the final mean calculation, in this example, only the last pixel (equals 0) wouldn't join the equation, once it used only the ones with values higher than 0.

Figure 2 - Resumed CCI implementation scheme. The original image (matrix) is normalized, and a mobile 3x3 kernel scrolls through the whole image, computing local standard deviations. Finally, the arithmetic mean of the pixels higher than zero is obtained.

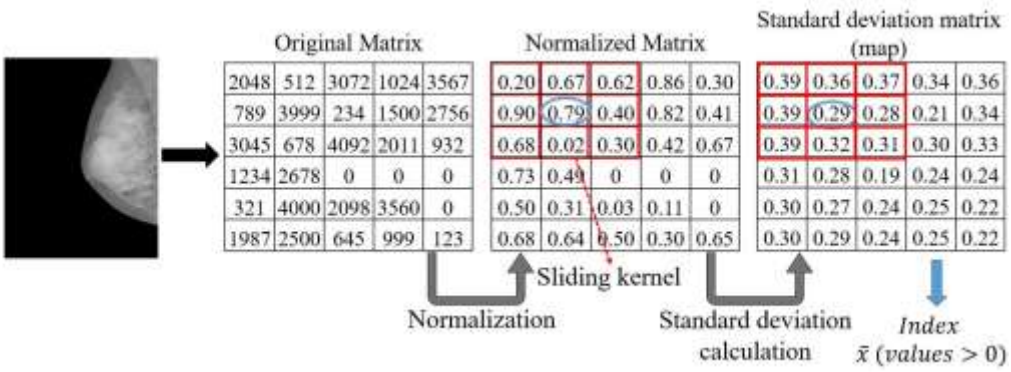

Source: Modified from [12].

Dataset

For this study, mammographic images from INbreast digital database were used in DICOM (Digital Imaging and Communications in Medicine) format [14]. This database comes from the *Hospitalar Center of São João*, in Porto, Portugal, where all images were obtained from the same digital mammograph, Siemens FFDM MammoNovation, with a contrast resolution of 12 bits. The size of the images depends on the compression (size) of the breast and can be either 3328x4084 or 2560x3328 pixels the medial-lateral oblique (MLO) and craniocaudal (CC) incidences.

For this first part, 98 exams labeled as dense breasts were selected. From all 98, 77 images belonged to category 'c' in terms of breast density, and the other 21 belonged to category 'd', the densest one, according to the BI-RADS ACR. Both breast types increase the diagnosis difficulty, reducing the sensibility of the mammographic exam. The selected images contained only microcalcifications as the main lesion, excluding the images with nodules, aiming to target the radiologists' analysis on the CLAHE technique effect in the image, once the presence of nodules might draw all attention to the enhancement produced by them. Table 1 resumes the total number of images and the respective amount of each incidence/positioning.

Table 1 – Part I: quantitative summary of the images, divided by incidence (positioning).

Breast density	Number of images (MLO/CC)
Category 'c'	77 (39/38)
Category 'd'	21 (11/10)
Total	98

Source: Modified from [16].

Image Processing

The CLAHE (Contrast-Limited Adaptive Histogram Equalization) was applied through MATLAB®, where each one of the 98 original images, previously selected, was processed. Figure 3 illustrates the CLAHE application process, using one of the used images as an example.

Figure 3 – (A) Example of mammographic image used in the present work; (B) Histogram of the original mammographic image; (C) Settled parameters, and in this example uniform distribution, number of subregions divisions equal to 3x3 and cut off limit equals 0.01 were used. (D) The pixels contained within the crop region are redistributed generating a new histogram, and a new resulting image after processing with CLAHE.

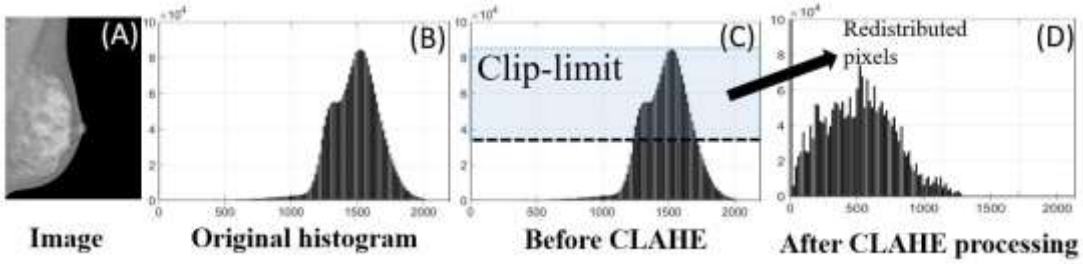

Source: Modified from [16].

Figure 4 presents the results of the images after the use of CLAHE technique, varying the parameters (cut off limit and function/probability distribution).

In short, the parameter used on CLAHE for the 98 images were:

- Clip-limit: 0.01;
- Distribution function: uniform;
- Subregion (window) sizes ranging from: 3x3, 5x5, 7x7, 9x9, 12x12 e 15x15;

For the quantitative evaluation of the images, EME and CCI values were calculated. For the EME calculus, an automatic ROI delimitation, of size 500x500 pixels, was implemented, along with the following methodology:

1. The central pixel of the image is calculated by dividing the size (m x n) of the image by 2;
2. Breast laterality is verified, aiming to select a region placed, obligatorily, inside the breast's useful area. That means that a breast with left laterality contains its useful information on the central pixel's left, whereas a breast with right laterality presents its useful information on the central pixel's right side;
3. The central pixel is moved in 750 columns to the left or to the right, depending on the breast's laterality;
4. This new spot is considered the central point to delimitate the 500x500 sized ROI, that will be used on the EME calculation.

Figure 4 – Variation of the cut off limit (0.01, 0.05 and 0.1), as well as the function used (exponential or uniform). It is noticeable that the cut off limit equals 0.05 and mainly 0.1, some regions of the image have saturated. For this work, a cut off limit equals 0.01 with uniform distribution was used, as shown in the first image of the second line.

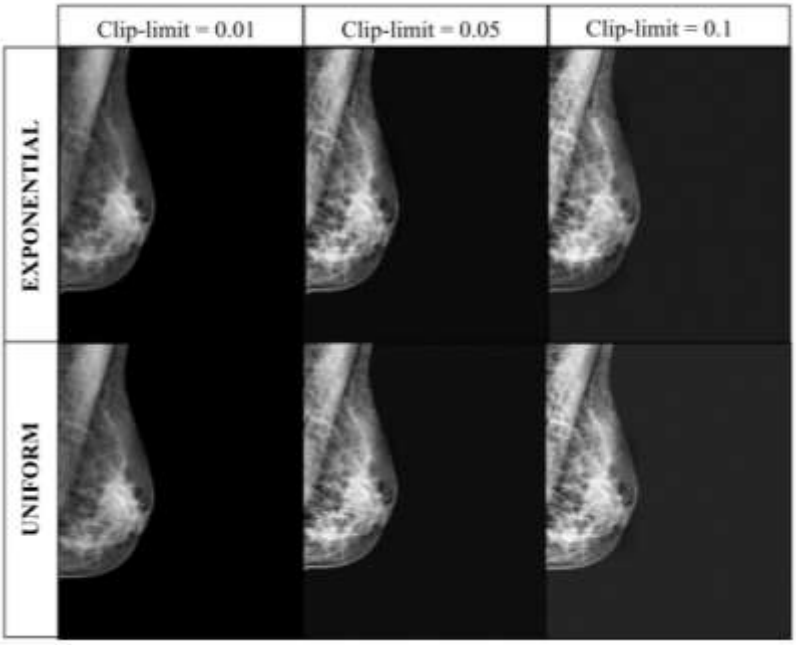

Source: Modified from [16].

Figure 5 exemplifies a ROI example extracted from the described methodology. It is notable that, on the example, the breast presents right laterality, therefore, the sliding kernel must be displaced to the right, making sure that the ROI is in an area containing information about the image. In this case, if the kernel was displaced to the left, the selected ROI would contemplate only black background pixels. The displacement in 750 columns assured that all the delimited regions of interest contained useful areas of the breast.

Figure 5 – Example of the region of interest (ROI) delimiting, with size 500x500 pixels cut from the image center point. The ROI is shifted to the left or right depending on breast laterality, always ensuring that the ROI is extracted from the useful area of the breast.

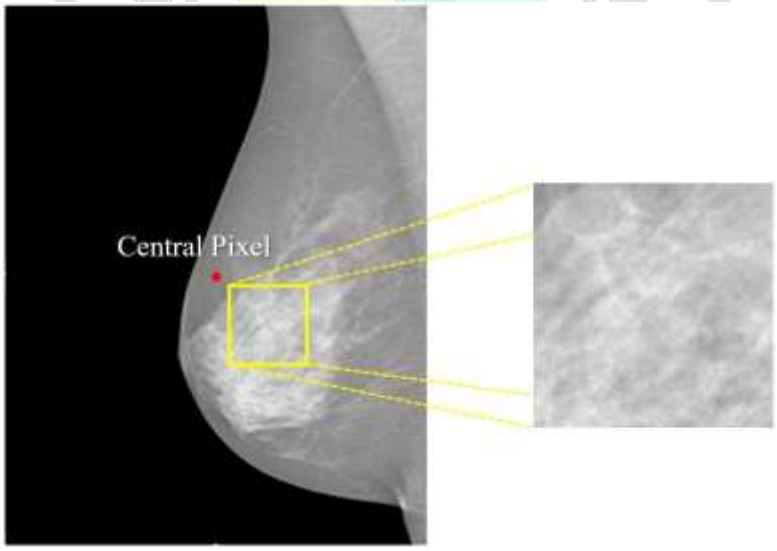

Source: Adapted from [12].

Finally, the Carneiro Contrast Index (CCI) was also calculated for all images, aiming to compare it to other contrast evaluation techniques. Before the CCI calculation, all images were submitted to a previous normalization process.

III. Results and Discussion

Based on previous studies [16] visual analysis, the two best processing techniques, as identified by a radiology specialist, were selected for metric application, specifically focusing on CLAHE. Therefore, Tables 2 and 3 display the results of the EME and CCI metrics, respectively.

According to the radiologist, the images with the best visual results were those that provided greater contrast between fibroglandular tissue and adjacent structures compared to the original images, which only included the acquisition equipment's pre-

processing. For most of the images evaluated by the radiologist, a subregion size of 15x15 pixels was selected [16]. Furthermore, when comparing the visual analysis results with the variance measure, it was noted that although higher values were obtained for 3x3 window images, this did not necessarily indicate visual improvement, despite the contrast increase. In other words, images processed with a 15x15 subregion size did not show the highest variance values. However, their mean variance values were higher than those of the original images, suggesting an increase in contrast, similar to the 3x3 window images, but with improved visual quality.

By the end of the quantitative metrics calculation for the breast images, the arithmetic mean of the images belonging to the same dataset and same processing was made, forming the results illustrated in Tables 2 and 3.

Table 2 - EME analysis results.

	EME ($\underline{\mu}\pm\sigma$)	
Processing method	**INbreast P3**	**INbreast P4**
1) CLAHE 3x3	4.50 ± 1.27	3.97 ± 1.18
2) CLAHE 15x15	7.89 ± 1.59	7.43 ± 1.44

Source: Modified from [12].

Table 3 - CCI analysis results.

	CCI ($\underline{\mu}\pm\sigma$)	
Processing method	**INbreast P3**	**INbreast P4**
1) CLAHE 3x3	10.03 ± 2.87	8.33 ± 1.96
2) CLAHE 15x15	11.43 ± 3.49	9.47 ± 2.13

Source: Modified from [12].

Some examples of processed images are shown in Figures 6 and Figure 7.

Figure 6 - Original craniocaudal category ‘c’ image (A), and its respective resultant images with different numbers of subregions applied: 3x3 (B), 5x5 (C), 7x7 (D), 9x9 (E), 12x12 (F), and 15x15 (G).

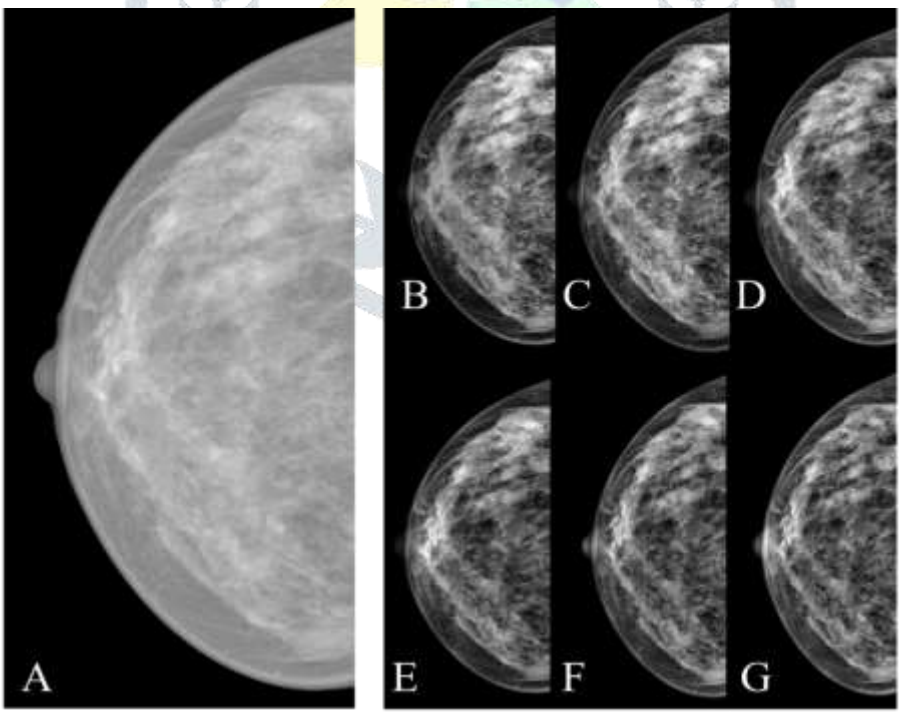

Source: [12].

Figure 7 - Original mediolateral oblique image category ‘d’ image (A) and its respective resultant images with different numbers of subregions applied: 3x3 (B), 5x5 (C), 7x7 (D), 9x9 (E), 12x12 (F), and 15x15 (G).

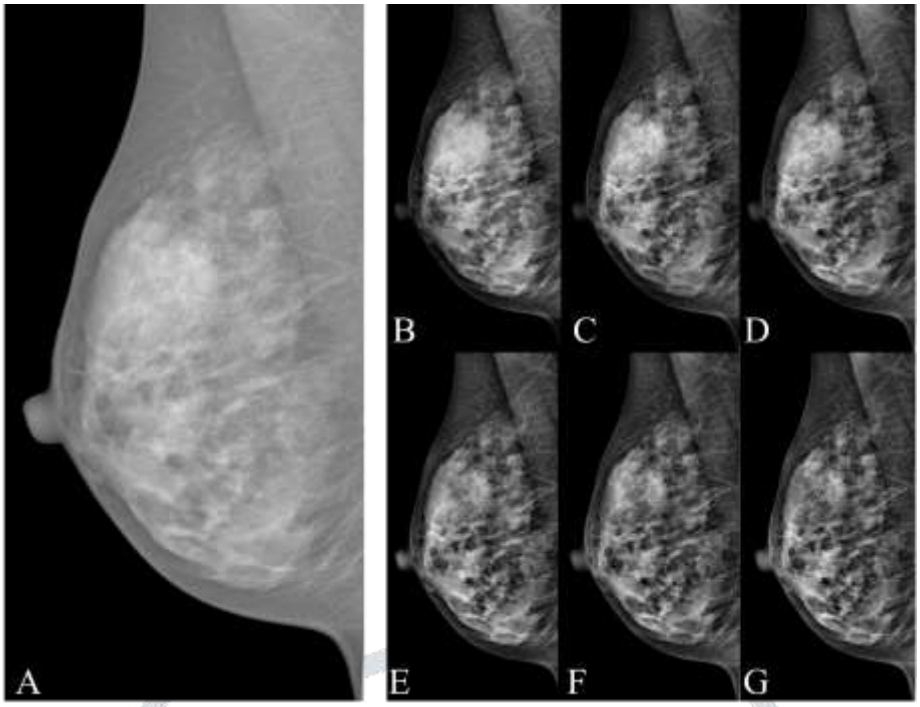

Source: [12].

Initially, the agreement between the CCI and EME values is verified in the original images. The proposed metric was based on the calculation of standard deviation values, once this measure is directly related to variance and, hence, to image contrast. The standard deviation represents the dispersion degree of a dataset, in this case, of the shades of gray in an image, and can also depict the uniformity level of the pixels. Thus, the higher the standard deviation, the higher the variance among the shades of gray of a region, indicating a greater numeric distance between pixels, therefore, suggesting higher contrast.

As well as for the EME, CCI coincided with the visual choice made by the radiologist, as shown in previous work [15]. The usage of CLAHE 15x15 in the image processing (with or without previous filtering) resulted in higher CCI values when compared to the same image processing using CLAHE 3x3.

Another result that helps validate CCI is the lower value obtained for images in category ‘d’, when compared to category ‘c’. Beyond the quantitative values, the CCI produces a map (image) from the local standard deviation values previously calculated by regions. Regions with higher contrast are represented in lighter shades in the map, while the regions with lower contrast tend to be darker in the resultant map. This shows the areas where the contrast enhancement was greater with the digital processing technique and helps identify possible findings in the images.

IV. Conclusion

The development and implementation of a new algorithm for measuring the global contrast of breast images have proven to be highly useful. In addition to expanding the range of contrast metrics, the CCI provides both a visual representation (standard deviation matrix) and a quantitative (numerical) result, making it applicable in various breast image analysis contexts.

Contrarily to EME, where a region of interest is required, CCI allows a whole image analysis, through the local standard deviation values. In summary, the proposed index calculates the arithmetic mean of standard deviation values greater than zero across all pixels in the target image.

The development of the Carneiro Contrast Index (CCI) represents an important contribution to the field of breast image analysis, providing a robust and objective method for evaluating contrast enhancement techniques. By allowing a global assessment of contrast without the need for predefined regions of interest, CCI ensures greater reproducibility and applicability in different imaging contexts. The results obtained demonstrate that the proposed metric aligns with both visual assessments by radiologists and existing contrast measures, reinforcing its reliability. Future studies may explore its integration with deep learning models and automated diagnostic systems, further enhancing the accuracy and efficiency of breast cancer detection.

REFERENCES

[1] GONZALEZ R.C., WOODS, R.E. (2007) Digital Image Processing. 3rd Edition, Pearson, London.

[2] MORROW, William Mark et al. Region-based contrast enhancement of mammograms. IEEE Transactions on Medical Imaging, v. 11, n. 3, p. 392-406, 1992. https://doi.org/10.1109/42.158944

[3] SAUNDERS JR, Robert S. et al. Does image quality matter? Impact of resolution and noise on mammographic task performance. Medical physics, v. 34, n. 10, p. 3971-3981, 2007. https://doi.org/10.1118/1.2776253

[4] CHENG, Heng-Da; XU, Huijuan. A novel fuzzy logic approach to contrast enhancement. Pattern Recognition, v. 33, n. 5, p. 809-819, 2000. https://doi.org/10.1016/S0031-3203(99)00096-5

[5] YOON, Jeong Hyun; RO, Yong Man. Enhancement of the contrast in mammographic images using the homomorphic filter method. IEICE Transactions on Information and Systems, v.85, n. 1, p. 298-303, 2002.

[6] MAKANDAR, Aziz; HALALLI, Bhagirathi. Breast cancer image enhancement using median filter and CLAHE. International Journal of Scientific & Engineering Research, v. 6, n. 4, p. 462-465, 2015.

[7] BHATEJA, Vikrant; MISRA, Mukul; UROOJ, Shabana. Human visual system based unsharp masking for enhancement of mammographic images. Journal of Computational Science, 2016. https://doi.org/10.1016/j.jocs.2016.07.015

[8] VIKHE, P. S.; THOOL, V. R. Contrast enhancement in mammograms using homomorphic filter technique. In: 2016 International Conference on Signal and Information Processing (IConSIP). IEEE, 2016. p. 1-5.

[9] SENTHILKUMAR, B. et al. Combination of noise removal and contrast enhancement methods for the preprocessing of mammogram images-towards the detection of breast cancer. Bioscience Journal, v. 33, n. 6, 2017. https://doi.org/10.14393/BJ-v33n6a2017-36020

[10] SAHU, Sima et al. An approach for de-noising and contrast enhancement of retinal fundus image using CLAHE. Optics & Laser Technology, v. 110, p. 87-98, 2019. https://doi.org/10.1016/j.optlastec.2018.06.061

[11] AKILA, K.; JAYASHREE, L. S.; VASUKI, A. Mammographic image enhancement using indirect contrast enhancement techniques–a comparative study. Procedia Computer Science, v. 47, p. 255-261, 2015. https://doi.org/10.1016/j.procs.2015.03.205

[12] CARNEIRO, Pedro Cunha. Proposta de metodologia para realce de contraste em imagens de mamas densas utilizando decomposição multiescala com transformada discreta wavelet. 2019. DOI https://doi.org/10.14393/ufu.te.2019.2593 .

[13] PERRY, N et al. European guidelines for quality assurance in breast cancer screening and diagnosis. Luxembourg: Office for official publications of the European Communities, 2006. 4th edition. https://doi.org/10.1093/annonc/mdm481

[14] BUSHBERG, Jerrold T.; BOONE, John M. The essential physics of medical imaging. Lippincott Williams & Wilkins, 2011.

[15] AGAIAN, Sos S.; PANETTA, Karen; GRIGORYAN, Artyom M. A new measure of image enhancement. In: IASTED International Conference on Signal Processing & Communication. 2000. p. 19-22.

[16] CARNEIRO, P. C. et al. CLAHE Parameters Effects on the Quantitative and Visual Assessment of Dense Breast Mammograms. IEEE Latin America Transactions, v. 17, n.5, p. 851-857, 2019. https://doi.org/10.1109/TLA.2019.8891954